The spatial calibration must be done at the same sample-to-detector distance as the diffraction-data collection.

2.5.3.3.3. *Frame integration*

2D frame integration is a data-reduction process which converts a two-dimensional frame into a one-dimensional intensity profile. Two forms of integration are generally of interest in the analysis of a 2D diffraction frame from polycrystalline materials: γ integration and 2θ integration. γ integration sums the counts in 2θ steps ($\Delta 2\theta$) along constant 2θ conic lines and between two constant γ values. γ integration produces a data set with intensity as a function of 2θ. 2θ integration sums the counts in γ steps ($\Delta\gamma$) along constant γ lines and between two constant 2θ conic lines. 2θ integration produces a data set with intensity as a function of γ. γ integration may also be carried out with the integration range in the vertical direction as a constant number of pixels. This type of γ integration may also be referred to as slice integration. A diffraction profile analogous to the conventional diffraction result can be obtained by either γ integration or slice integration over a selected 2θ range. Phase ID can then be done with conventional search/match methods. 2θ integration is of interest for evaluating the intensity variation along γ angles, such as for texture analysis, and is discussed in more depth in Chapter 5.3.

The γ integration can be expressed as

$$I(2\theta) = \int_{\gamma_1}^{\gamma_2} J(2\theta, \gamma)\, \mathrm{d}\gamma, \quad 2\theta_1 \leq 2\theta \leq 2\theta_2, \tag{2.5.23}$$

where $J(2\theta, \gamma)$ represents the two-dimensional intensity distribution in the 2D frame and $I(2\theta)$ is the integration result as a function of intensity *versus* 2θ. γ_1 and γ_2 are the lower limit and upper limit of integration, respectively, which are constants for γ integration. Fig. 2.5.13 shows a 2D diffraction frame collected from corundum (α-Al_2O_3) powder. The 2θ range is from 20 to 60° and the 2θ integration step size is 0.05°. The γ-integration range is from 60 to 120°. In order to reduce or eliminate the dependence of the integrated intensity on the integration interval, the integrated value at each 2θ step is normalized by the number of pixels, the arc length or the solid angle. γ integration with normalization by the solid angle can be expressed as

$$I(2\theta) = \frac{\int_{\gamma_1}^{\gamma_2} J(2\theta, \gamma)(\Delta 2\theta)\, \mathrm{d}\gamma}{\int_{\gamma_1}^{\gamma_2} (\Delta 2\theta)\, \mathrm{d}\gamma}, \quad 2\theta_1 \leq 2\theta \leq 2\theta_2. \tag{2.5.24}$$

Since the $\Delta 2\theta$ step is a constant, the above equation becomes

$$I(2\theta) = \frac{\int_{\gamma_1}^{\gamma_2} J(2\theta, \gamma)\, \mathrm{d}\gamma}{\gamma_2 - \gamma_1}, \quad 2\theta_1 \leq 2\theta \leq 2\theta_2. \tag{2.5.25}$$

There are many integration software packages and algorithms available for reducing 2D frames into 1D diffraction patterns for polycrystalline materials (Cervellino *et al.*, 2006; Rodriguez-Navarro, 2006; Boesecke, 2007). With the availability of tremendous computer power today, a relatively new method is the bin method, which treats pixels as having a continuous distribution in the detector. It demands more computer power than older methods, but delivers much more accurate and smoother results even with $\Delta 2\theta$ integration steps significantly smaller than the pixel size. Depending on the relative size of $\Delta 2\theta$ to the pixel size, each contributing pixel is divided into several 2θ 'bins'. The intensity counts of all pixels within the $\Delta 2\theta$ step are summarized. All the normalization methods in the above integration, either by pixel, arc or solid angle, result in an intensity level of one pixel or unit solid angle. Since a pixel is much smaller than the active area of a typical point detector, the normalized integration tends to result in a diffraction pattern with fictitiously low intensity counts, even though the true counts in the corresponding $\Delta 2\theta$ range are significantly higher. In order to avoid this misleading outcome, it is reasonable to introduce a scaling factor. However, there is no accurate formula for making the integrated profile from a 2D frame comparable to that from a conventional point-detector scan. The best practice is to be aware of the differences and to try not to make direct comparisons purely based on misleading intensity levels. Generally speaking, for the same exposure time, the total counting statistics from a 2D detector are significantly better than from a 0D or 1D detector.

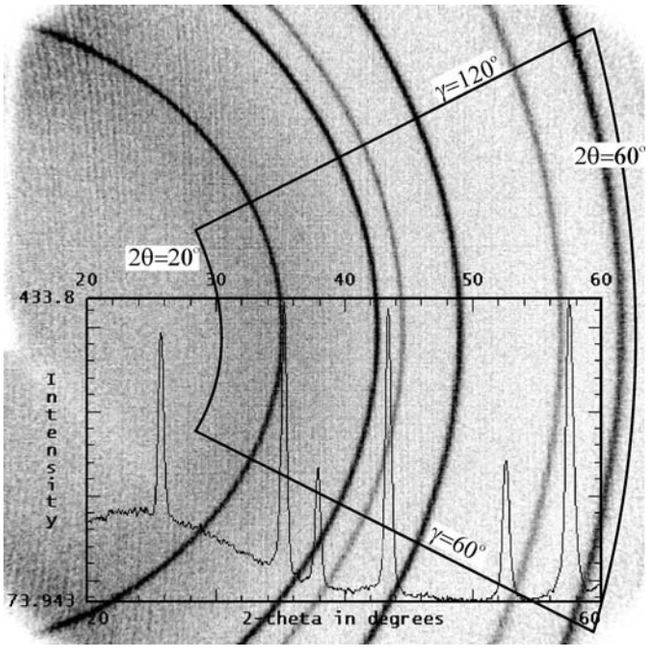

Figure 2.5.13
A 2D frame showing γ integration.

2.5.3.3.4. *Lorentz, polarization and absorption corrections*

Lorentz and polarization corrections may be applied to the diffraction frame to remove their effect on the relative intensities of Bragg peaks and background. The 2θ angular dependence of the relative intensity is commonly given as a Lorentz–polarization factor, which is a combination of Lorentz and polarization factors. In 2D diffraction, the polarization factor is a function of both 2θ and γ, therefore it should be treated in the 2D frames, while the Lorentz factor is a function of 2θ only. The Lorentz correction can be done either on the 2D frames or on the integrated profile. In order to obtain relative intensities equivalent to a conventional diffractometer with a point detector, reverse Lorentz and polarization corrections may be applied to the frame or integrated profile.

The Lorentz factor is the same as for a conventional diffractometer. For a sample with a completely random orientation distribution of crystallites, the Lorentz factor is given as

$$L = \frac{\cos\theta}{\sin^2 2\theta} = \frac{1}{4\sin^2\theta\cos\theta}. \tag{2.5.26}$$

The Lorentz factor may be given by a different equation for a different diffraction geometry (Klug & Alexander, 1974). The forward and reverse Lorentz corrections are exactly reciprocal

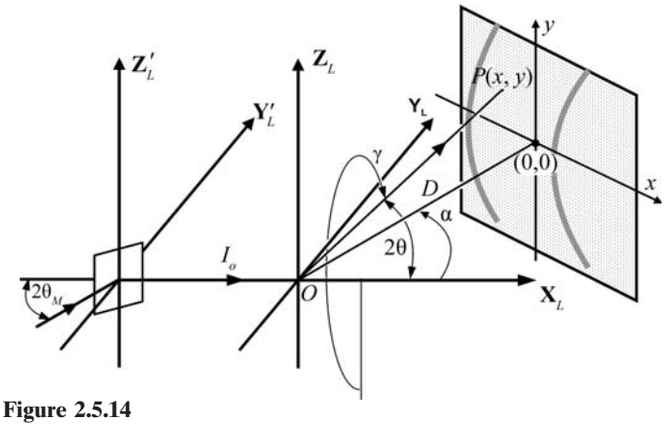

Figure 2.5.14
Geometric relationship between the monochromator and detector in the laboratory coordinates.

and effectively cancel each other. Therefore, it is not necessary to perform the Lorentz correction to the frame before integration if relative intensities equivalent to a conventional Bragg–Brentano diffractometer are expected. The Lorentz correction can be done on the integrated diffraction profiles in the same way as on the diffraction profiles collected with conventional diffractometers.

When a non-polarized X-ray beam is scattered by matter, the scattered X-rays are polarized. The intensity of the diffracted beam is affected by the polarization; this effect is expressed by the polarization factor. In two-dimensional X-ray diffraction the diffraction vectors of the monochromator diffraction and sample crystal diffraction are not necessarily in the same plane or perpendicular planes. Therefore, the overall polarization factor is a function of both 2θ and γ. Fig. 2.5.14 illustrates the geometric relationship between the monochromator and detector in the laboratory coordinates, X_L, Y_L, Z_L. The monochromator is located at the coordinates X_L, Y'_L, Z'_L, which is a translation of the laboratory coordinates along the X_L axis in the negative direction. The monochromator crystal is rotated about the Z'_L axis and $2\theta_M$ is the Bragg angle of the monochromator crystal. The diffracted beam from the monochromator propagates along the X_L direction. This is the incident beam to the sample located at the instrument centre O. The 2D detector location is given by the sample-to-detector distance D and swing angle α. The pixel $P(x, y)$ represents an arbitrary pixel on the detector. 2θ and γ are the corresponding diffraction-space parameters for the pixel. Since a monochromator or other beam-conditioning optics can only be used on the incident beam, the polarization factor for 2D-XRD can then be given as a function of both θ and γ:

$$P(\theta, \gamma) = \frac{(1 + \cos^2 2\theta_M \cos^2 2\theta)\sin^2\gamma + (\cos^2 2\theta_M + \cos^2 2\theta)\cos^2\gamma}{1 + \cos^2 2\theta_M}. \quad (2.5.27)$$

If the crystal monochromator rotates about the Y'_L axis, *i.e.* the incident plane is perpendicular to the diffractometer plane, the polarization factor for two-dimensional X-ray diffraction can be given as

$$P(\theta, \gamma) = \frac{(1 + \cos^2 2\theta_M \cos^2 2\theta)\cos^2\gamma + (\cos^2 2\theta_M + \cos^2 2\theta)\sin^2\gamma}{1 + \cos^2 2\theta_M}. \quad (2.5.28)$$

In the above equations, the term $\cos^2 2\theta_M$ can be replaced by $\left|\cos^n 2\theta_M\right|$ for different monochromator crystals. For a mosaic crystal, such as a graphite crystal, $n = 2$. For most real monochromator crystals, the exponent n takes a value between 1 and 2. For near perfect monochromator crystals, n approaches 1 (Kerr & Ashmore, 1974). All the above equations for polarization factors may apply to multilayer optics. However, since multilayer optics have very low Bragg angles, $\left|\cos^n 2\theta_M\right|$ approximates to unity. The γ dependence of the polarization factor diminishes in this case. The polarization factor approaches

$$P(\theta, \gamma) \simeq \frac{1 + \cos^2 2\theta}{2}. \quad (2.5.29)$$

2.5.3.3.5. *Air scatter*

X-rays are scattered by air molecules in the beam path between the X-ray source and detector. Air scatter results in two effects: one is the attenuation of the X-ray intensity, the other is added background in the diffraction pattern. Air scatter within the enclosed primary beam path – for instance, in the mirror, monochromator housing or collimator – results in attenuation of only the incident beam. The enclosed beam path can be purged by helium gas or kept in vacuum to reduce the attenuation so that no correction is necessary for this part of the air scatter. The open beam between the tip of the collimator and the sample generates an air-scatter background pattern, which is the major part of the air scatter. In the secondary beam path, the air scatter from the diffracted beam may generate background too, but the main effect of the air scatter is inhomogeneous attenuation of the diffraction pattern due to the different beam path lengths between the centre and the edge of the detector.

The background generated by air scattering from the open incident-beam path has a strong 2θ dependence. The specific scattering curve depends on the length of the open primary beam path, the beam size and the wavelength of the incident beam. There are two approaches to correct air scatter. One is to collect an air-scatter background frame under the same conditions as the diffraction frame except without a sample. The background frame is then subtracted from the diffraction frame. Another approach is to remove the background from the integrated profile, since the background is 2θ dependent.

The attenuation of the diffracted beam by air absorption depends on the distance between the sample and pixel. For a flat detector, air absorption can be corrected by

$$p_c(x, y) = p_o(x, y)\exp\left[\mu_{\rm air}(D^2 + x^2 + y^2)^{1/2}\right], \quad (2.5.30)$$

where $p_o(x, y)$ is the original pixel intensity of the pixel $P(x, y)$ and $p_c(x, y)$ is the corrected intensity. The detector centre is given by $(0, 0)$. $\mu_{\rm air}$ is the linear absorption coefficient of air. The value of $\mu_{\rm air}$ is determined by the radiation wavelength. By approximation, for air with 80% N_2 and 20% O_2 at sea level and at 293 K, $\mu_{\rm air}$ = 0.01 cm^{-1} for Cu $K\alpha$ radiation. Air scatter and absorption increases with increasing wavelength. For example, $\mu_{\rm air}$ = 0.015 cm^{-1} for Co $K\alpha$ radiation and 0.032 cm^{-1} for Cr $K\alpha$ radiation. The absorption coefficient for Mo $K\alpha$ radiation, $\mu_{\rm air}$ = 0.001 cm^{-1}, is only one-tenth of that for Cu $K\alpha$ radiation, so an air-absorption correction is not necessary. Alternatively, the absorption correction may be normalized to the absorption level in the beam centre as

$$p_c(x, y) = p_o(x, y)\exp\left\{\mu_{\rm air}\left[(D^2 + x^2 + y^2)^{1/2} - D\right]\right\}. \quad (2.5.31)$$